Cancer Cell
Article

A Mitochondria-K^+ Channel Axis Is Suppressed in Cancer and Its Normalization Promotes Apoptosis and Inhibits Cancer Growth

Sébastien Bonnet,[1] Stephen L. Archer,[1,2] Joan Allalunis-Turner,[3] Alois Haromy,[1] Christian Beaulieu,[4] Richard Thompson,[4] Christopher T. Lee,[5] Gary D. Lopaschuk,[5,6] Lakshmi Puttagunta,[7] Sandra Bonnet,[1] Gwyneth Harry,[1] Kyoko Hashimoto,[1] Christopher J. Porter,[8] Miguel A. Andrade,[8] Bernard Thebaud,[1,6] and Evangelos D. Michelakis[1,*]

[1] Pulmonary Hypertension Program and Vascular Biology Group
[2] Department of Physiology
[3] Department of Oncology
[4] Department of Biomedical Engineering
[5] Department of Pharmacology
[6] Department of Pediatrics
[7] Department of Laboratory Medicine and Pathology
University of Alberta, Edmonton, AB T6G 2B7, Canada
[8] Ontario Genomics Innovation Centre, Ottawa Health Research Institute, and Department of Cellular and Molecular Medicine, University of Ottawa, Ottawa, ON K1N 6N5, Canada
*Correspondence: emichela@cha.ab.ca
DOI 10.1016/j.ccr.2006.10.020

SUMMARY

The unique metabolic profile of cancer (aerobic glycolysis) might confer apoptosis resistance and be therapeutically targeted. Compared to normal cells, several human cancers have high mitochondrial membrane potential ($\Delta\Psi m$) and low expression of the K^+ channel Kv1.5, both contributing to apoptosis resistance. Dichloroacetate (DCA) inhibits mitochondrial pyruvate dehydrogenase kinase (PDK), shifts metabolism from glycolysis to glucose oxidation, decreases $\Delta\Psi m$, increases mitochondrial H_2O_2, and activates Kv channels in all cancer, but not normal, cells; DCA upregulates Kv1.5 by an NFAT1-dependent mechanism. DCA induces apoptosis, decreases proliferation, and inhibits tumor growth, without apparent toxicity. Molecular inhibition of PDK2 by siRNA mimics DCA. The mitochondria-NFAT-Kv axis and PDK are important therapeutic targets in cancer; the orally available DCA is a promising selective anticancer agent.

INTRODUCTION

Cancer progression and its resistance to treatment depend, at least in part, on suppression of apoptosis. Although mitochondria are recognized as regulators of apoptosis, their importance as targets for cancer therapy has not been adequately explored or clinically exploited. In 1930, Warburg suggested that mitochondrial dysfunction in cancer results in a characteristic metabolic phenotype, that is, aerobic glycolysis (Warburg, 1930). Positron emission tomography (PET) imaging has now confirmed that most malignant tumors have increased glucose uptake and metabolism. This bioenergetic feature is a good marker of cancer but has not been therapeutically pursued, as it

SIGNIFICANCE

The small molecule DCA is a metabolic modulator that has been used in humans for decades in the treatment of lactic acidosis and inherited mitochondrial diseases. Without affecting normal cells, DCA reverses the metabolic-electrical remodeling that we describe in several cancer lines (hyperpolarized mitochondria, activated NFAT1, downregulated Kv1.5), inducing apoptosis and decreasing tumor growth. DCA in the drinking water at clinically relevant doses for up to 3 months prevents and reverses tumor growth in vivo, without apparent toxicity and without affecting hemoglobin, transaminases, or creatinine levels. The ease of delivery, selectivity, and effectiveness make DCA an attractive candidate for proapoptotic cancer therapy which can be rapidly translated into phase II–III clinical trials.

is thought to be a result and not a cause of cancer; that is, the cells rely mostly on glycolysis for energy production because of permanent mitochondrial damage, preventing oxidative phosphorylation. However, whether the mitochondria in cancer are indeed damaged and whether this is reversible remain unknown.

The metabolic hypothesis of cancer has recently been rekindled. Gatenby and Gillies recently proposed that because early carcinogenesis occurs in a hypoxic microenvironment, the transformed cells initially have to rely on glycolysis for energy production (Gatenby and Gillies, 2004). However, this early metabolic adaptation appears to also offer a proliferative advantage, suppressing apoptosis. Furthermore, the "byproducts" of glycolysis (i.e., lactate and acidosis) contribute to the breakdown of the extracellular matrix, facilitate cell mobility, and increase the metastatic potential. Therefore, even though the tumors eventually become vascularized and O_2 levels increase, the glycolytic phenotype persists, resulting in the "paradox" of glycolysis during aerobic conditions (the Warburg effect). Metabolic and apoptotic pathways that converge in the mitochondria are not independent from each other, and it appears that glycolytic phenotype is indeed associated with a state of apoptosis resistance (Plas and Thompson, 2002). Many glycolytic enzymes have been recognized to also regulate apoptosis, and several oncoproteins induce the expression of glycolytic enzymes (Kim and Dang, 2005). For example, Akt, which stimulates glycolysis and induces resistance to apoptosis (Elstrom et al., 2004), activates hexokinase, an enzyme catalyzing the first and irreversible step in glycolysis. Via its downstream mediator glycogen synthase kinase 3 (GSK3), Akt induces the translocation of hexokinase to the mitochondrial membrane where it binds to the voltage-dependent anion channel (VDAC), suppressing apoptosis (Kim and Dang, 2005; Pastorino et al., 2005). Inhibition of GSK3 in cancer cells causes unbinding of hexokinase from VDAC, induces apoptosis, and increases sensitivity to chemotherapy (Pastorino et al., 2005). This suggests that perhaps the metabolic phenotype in cancer is due to a potentially plastic mitochondrial remodeling that results in suppressed oxidative phosphorylation, enhanced glycolysis, and suppressed apoptosis.

Whether the metabolism of glucose will end with glycolysis in the cytoplasm (converting pyruvate to lactate) or continue with glucose oxidation in the mitochondria is controlled by a gate-keeping mitochondrial enzyme, pyruvate dehydrogenase (PDH) (Figure 1). PDH converts pyruvate to acetyl-CoA which, along with the acetyl-CoA from the fatty acid β-oxidation, is fed to the Krebs cycle, producing the electron donors NADH and $FADH_2$. NADH donates electrons to complex I of the electron transport chain (ETC) (and $FADH_2$ to complex III). The flux of electrons down the ETC is associated with production of reactive oxygen species (ROS) and with the efflux of H^+, which causes a negative mitochondrial membrane potential ($\Delta\Psi m$). The F1F0-ATP synthase uses the stored energy of the $\Delta\Psi m$ to synthesize ATP; thus the $\Delta\Psi m$ reflects ETC activity and mitochondrial function. PDH is inhibited by phosphorylation by PDH kinase (PDK). The role of PDH and PDK in cancer is unknown.

Mitochondrial remodeling has multiple downstream effects, beyond energy production, because mitochondria regulate several critical functions including $[Ca^{2+}]_i$ and ROS-redox control. Through the release of ROS, mitochondria regulate the opening of plasma-membrane ion channels and through the control of $[Ca^{2+}]_i$, regulate Ca^{2+}-sensitive transcription factors. Some of these downstream pathways are also important in apoptosis and might contribute to the apoptosis resistance in cancer. For example, inhibition or downregulation of K^+ channels results in increased $[K^+]_i$, by decreasing the tonic efflux of K^+ down its intracellular/extracellular gradient (145/5 mEq). Because $[K^+]_i$ exerts a tonic inhibitory effect on caspases, K^+ channel inhibition or downregulation suppresses apoptosis in several cell types, including cancer (Andersson et al., 2006; Remillard and Yuan, 2004; Wang et al., 2002; Yu et al., 1997). The voltage-gated family of K^+ channels (Kv) is redox sensitive and therefore can be regulated by mitochondria. For example, mitochondria-derived H_2O_2 (a relatively stable ROS) can activate Kv1.5 (Caouette et al., 2003). Furthermore, the mitochondria-derived proapoptotic mediator cytochrome *c* activates, whereas the antiapoptotic bcl-2 inhibits, Kv channels (Remillard and Yuan, 2004). This mitochondria-ROS-Kv channel axis is now recognized as a basis of an important O_2-sensing mechanism in many tissues (Michelakis et al., 2004).

In preliminary experiments, we compared several cancer with normal cell lines and found that cancer cells had more hyperpolarized mitochondria and were relatively deficient in Kv channels. If this metabolic-electrical remodeling is an adaptive response, then its reversal might increase apoptosis and inhibit cancer growth. We used dichloroacetate (DCA), a small, orally available small molecule and a well-characterized inhibitor of PDK (Bowker-Kinley et al., 1998; Knoechel et al., 2006; Stacpoole, 1989). As seen in Figure 1, inhibition of PDK shifts pyruvate metabolism from glycolysis and lactate production to glucose oxidation in the mitochondria. The ability of DCA to decrease lactate production has been used for more than 30 years in the treatment of lactic acidosis that complicates inherited mitochondrial diseases in humans (Stacpoole et al., 1988, 2006).

We hypothesized that the downstream effects of the DCA-induced shift in metabolism will have beneficial effects in cancer therapy (Figure 1). We show that, as predicted, DCA changes the metabolism of cancer cells from the cytoplasm-based glycolysis to the mitochondria-based glucose oxidation. This is associated with increased production of ROS and decreased $\Delta\Psi m$ in all cancer, but not normal, cells, efflux of proapoptotic mediators from the mitochondria, and induction of mitochondria-dependent apoptosis. DCA also reverses the inhibition and downregulation of Kv1.5 in all cancer, but not normal, cells. The resultant efflux of K^+, and decrease in intracellular K^+, further increases the proapoptotic effects of DCA. DCA effectively decreases tumor growth in vitro

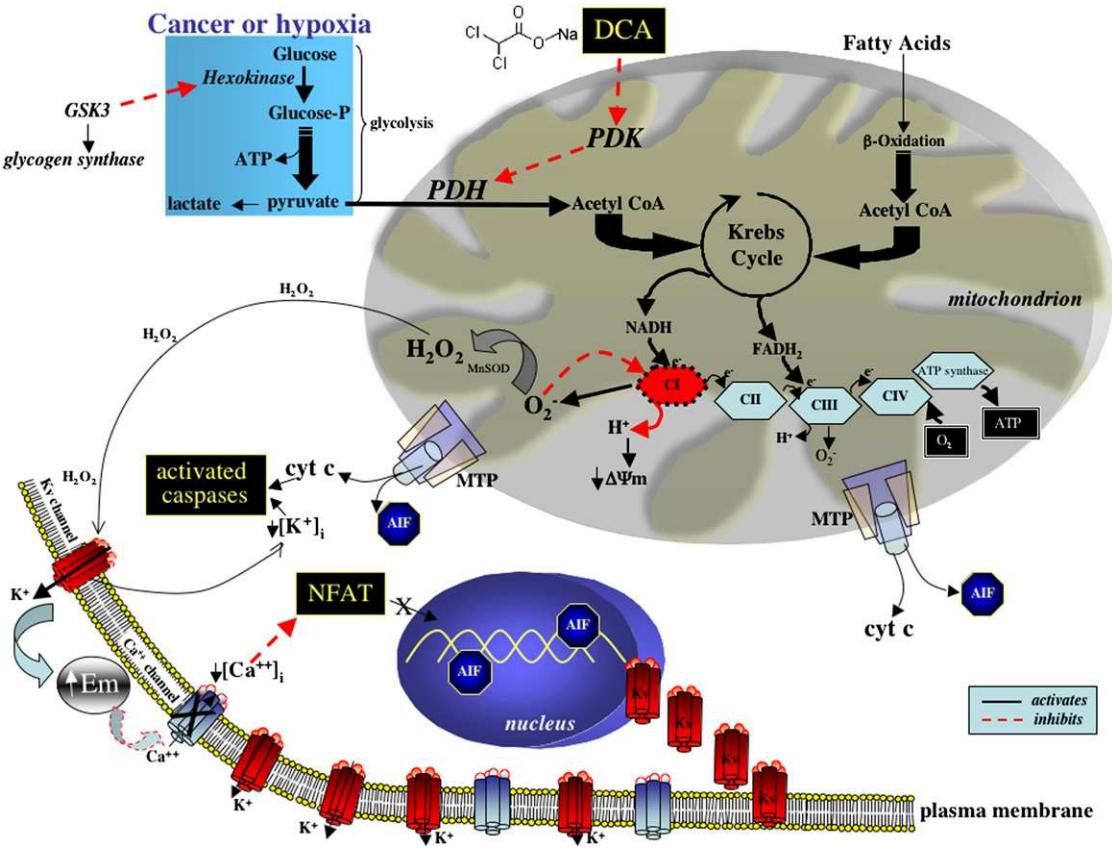

Figure 1. A Reversible Metabolic-Electrical Remodeling in Cancer Contributes to Resistance to Apoptosis and Reveals Several Potential Therapeutic Targets

In cancer, mitochondrial glucose oxidation is inhibited and energy production relies on the cytoplasmic glycolysis. This "inactivity" of the mitochondria likely induces a state of apoptosis resistance. Activation of PDH by DCA increases glucose oxidation by promoting the influx of acetyl-CoA into the mitochondria and the Krebs cycle, thus increasing NADH delivery to complex I of the electron transport chain, increasing the production of superoxide, which in the presence of MnSOD is dismutated to the more stable H_2O_2. Sustained increase in ROS generation can damage the redox-sensitive complex I, inhibiting H^+ efflux and decreasing $\Delta\Psi m$. Opening of the $\Delta\Psi m$-sensitive mitochondrial transition pore (MTP) allows the efflux of cytochrome *c* and apoptosis inducing factor (AIF). Both cytochrome *c* and H_2O_2 open the redox-sensitive K^+ channel Kv1.5 in the plasma membrane and hyperpolarize the cell (increased Em), inhibiting a voltage-dependent Ca^{2+} entry. The decreased $[Ca^{2+}]_i$ suppresses a tonic activation of NFAT, resulting in its removal from the nucleus, thus increasing Kv1.5 expression. The increased efflux of K^+ from the cell decreases the tonic inhibition of $[K^+]_i$ on caspases, further enhancing apoptosis. DCA's selectivity is based on its ability to target the unique metabolic profile that characterizes most cancers, and its effectiveness is explained by its dual mechanism of apoptosis induction, both by depolarizing mitochondria (proximal pathway) and activating/upregulating Kv1.5 (distal pathway).

and in vivo. We show that a metabolic-electrical remodeling regulates apoptosis resistance in cancer. Moreover, this abnormality is easily reversible by a simple drug that is already used in humans.

RESULTS

Cancer Mitochondria Are Hyperpolarized and Have Suppressed Oxidative Metabolism, Both of which Are Reversed by DCA

We studied $\Delta\Psi m$ in three human cancer cell lines: A549 (non-small-cell lung cancer), M059K (glioblastoma), and MCF-7 (breast cancer), and compared them with healthy, noncancerous human cell lines: small airway epithelial cells (SAEC), fibroblasts, and pulmonary artery smooth muscle cells (PASMC). All cancer cell lines had significantly more hyperpolarized $\Delta\Psi m$ compared to normal cells (increased fluorescence of the $\Delta\Psi m$-sensitive positive dye tetramethyl rhodamine methyl ester; TMRM). Incubation of all three types of cancer cells with DCA (48 hr) reversed the hyperpolarization and returned the $\Delta\Psi m$ to the level of the normal cells ($n \sim 80$ cells, 10 plates/cell line/group). In contrast, DCA did not alter the $\Delta\Psi m$ of the SAEC (Figure 2A), fibroblasts, and PASMC (not shown). The DCA effects on mitochondrial $\Delta\Psi m$ occurred as quickly as 5 min and were dose dependent (Figure 2B). Because the intracellular distribution of TMRM can theoretically be affected by differences in the plasma-membrane potential (Em), we used a protonophore (carbonylcyanide-*p*-trifluoromethoxyphenylhydrazone; FCCP) and showed that in all cancer cell lines it decreased $\Delta\Psi m$ in a dose-dependent manner, eventually depolarizing untreated and

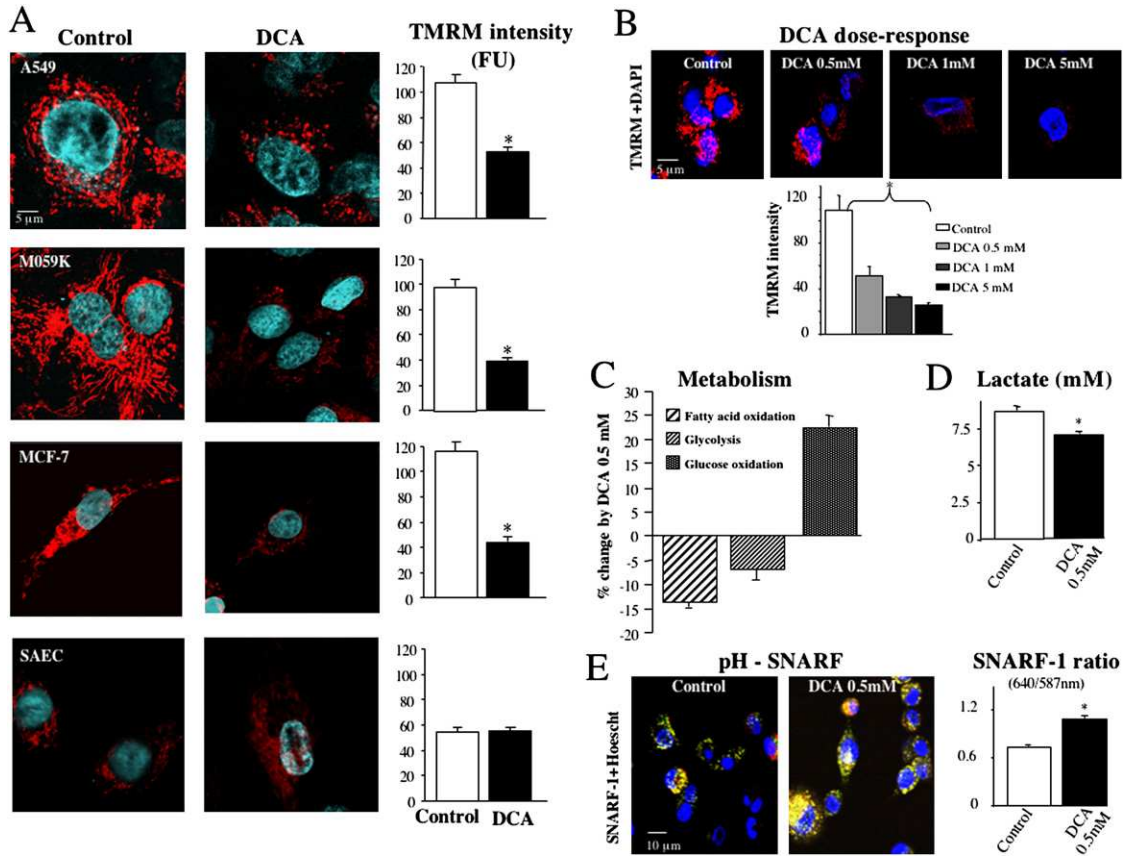

Figure 2. DCA Reverses the Glycolytic Phenotype and Depolarizes Mitochondria in Cancer, but Not Healthy, Cells

(A) Forty-eight hours of DCA (0.5 mM) significantly depolarized A549, MO59K, and MCF-7 cancer cells, but had no effect on healthy SAEC.

(B) DCA depolarizes mitochondria acutely (5–10 min) and in a dose-dependent manner.

(C) DCA increases glucose oxidation and suppresses glycolysis and fatty acid oxidation in A549 cells.

(D and E) Forty-eight hours of DCA (0.5 mM) decreased extracellular lactate levels and increased pH in A549 cells, measured by the SNARF-1 ratiometric dye.

*$p < 0.05$ versus control.

DCA-treated cells at the same low $\Delta\Psi m$ (see Figure S1 in the Supplemental Data available with this article online). This suggests that the TMRM signal was not confounded by DCA effects on the Em, but was rather due to true changes in the $\Delta\Psi m$.

To determine the effect of DCA on metabolism, we measured glycolysis (Gl), glucose oxidation (GO), and fatty acid oxidation (FAO) in A549 cells (10 plates/experiment, n = 3). DCA significantly increased GO rates (+23%), with a concomitant decrease in both Gl and FAO (Figure 2C). As expected from the DCA-induced shift of pyruvate metabolism away from lactate and toward acetyl-CoA and the Krebs cycle, the lactic-acid levels in the culture medium of the DCA-treated cells decreased (Figure 2D, n = 10 plates/group) and the intracellular pH increased (Figure 2E, n = 5 plates, 60 cells/group).

DCA Causes Efflux of Proapoptotic Factors from Mitochondria and Increases ROS Production

Whereas the untreated cancer cells (A549) showed cytochrome *c* and apoptosis-inducing factor (AIF) restricted to the mitochondria (colocalized with mitotracker red), in the DCA-treated cells cytochrome *c* was diffusely present in the cytoplasm and AIF was translocated to the nucleus (Figure 3A), both indicating induction of apoptosis.

DCA increased H_2O_2 production in a dose-dependent manner; this increase was inhibited by rotenone, suggesting that it was based on complex I of the ETC (Figure 3B, n = 5 plates/group). We also measured NADH levels in isolated mitochondria and showed that DCA increased the intramitochondrial NADH (Figure 3C, 5 plates/experiment, n = 5). The DCA-induced decrease in $\Delta\Psi m$ was limited by the VDAC (an important component of the mitochondrial transition pore; MTP) inhibitor 4′-diisothiocyano-2,2′-disulfonic acid stilbene (DIDS; 0.5 mM) (Granville and Gottlieb, 2003) (Figure 3D, n = 5, ~60 cells/group).

To determine whether cancer cells are less dependent on the ETC and oxidative phosphorylation, we studied the effects of low-dose cyanide (a complex-IV inhibitor and a well-known poison for normal cells). Cyanide's effects on mitochondria (as measured by $\Delta\Psi m$) were

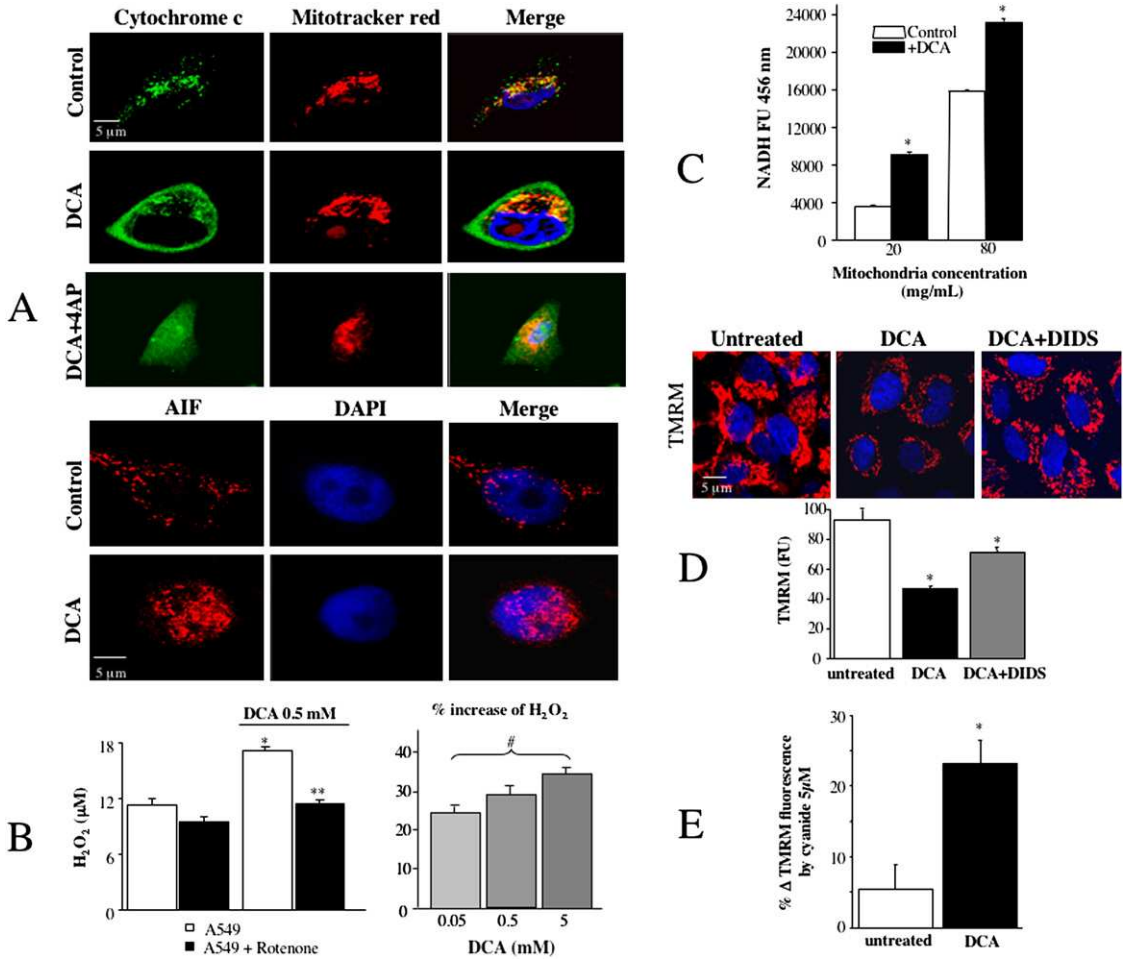

Figure 3. DCA Opens the MTP, Increases Intramitochondrial NADH and H_2O_2 Production, and Induces Mitochondrial Apoptosis in A549 Cells

(A) Cytochrome *c* in green is colocalized with the mitotracker red staining in untreated cancer cells, whereas after 48 hr of DCA (0.5 mM) treatment, cytochrome *c* leaks out of the mitochondria into the cytosol. In DCA-treated cells, apoptosis-inducing factor (AIF, red) is mainly localized in the nucleus (i.e., activated), in contrast to the untreated A549 cells.

(B) DCA increases H_2O_2 production (*$p < 0.05$) in a dose-dependent manner (#$p < 0.05$), and this is almost completely inhibited by rotenone (5 μM) (**$p < 0.05$), an inhibitor of mitochondrial electron transport chain complex I.

(C) DCA increases the intramitochondrial NADH in mitochondria isolated from untreated control and DCA-treated A549 cells (48 hr, 0.5 mM) (*$p < 0.05$).

(D) The DCA-induced mitochondrial depolarization is inhibited by DIDS, an inhibitor of the mitochondrial VDAC, which is a critical component of MTP (*$p < 0.05$).

(E) Cyanide (5 μM) does not affect mitochondrial function ($\Delta\Psi m$) in cancer cells significantly, in contrast to the DCA-treated cells, supporting the relative independence of cancer cells from the mitochondrial ETC (*$p < 0.05$).

much less pronounced in cancer compared to the DCA-treated cells (Figure 3E, n = 5, ~60 cells/group).

DCA Activates Kv Channels in Cancer Cells by an H_2O_2-Dependent Mechanism

Using whole-cell patch clamping, we showed that in all untreated cancer cell lines the outward K^+ current (Ik) was small and essentially voltage independent. DCA increased the Ik significantly in all cancer cell lines, but did not alter the Ik in the noncancerous SAEC (Figure 4A), PASMC, or fibroblasts (not shown) (Figure 4A, n = 7–8/group). The increase in Ik occurred as early as 5 min and persisted after 48 hr of DCA exposure. Most of the increased Ik was voltage dependent and blocked by 4-aminopyridine, a specific Kv channel inhibitor. The increased Ik caused hyperpolarization of the plasma-membrane Em. DCA also decreased cell capacitance, an electrophysiologic surrogate of cell size/volume, consistent with the cell shrinkage that characterizes early apoptosis (Figure 4A).

The DCA-induced increase in Ik was blocked by intracellular catalase, delivered through the patch pipette (i.e., due to H_2O_2), and by rotenone (i.e., due to complex I-produced H_2O_2), but not by thenoyltrifluoroacetone

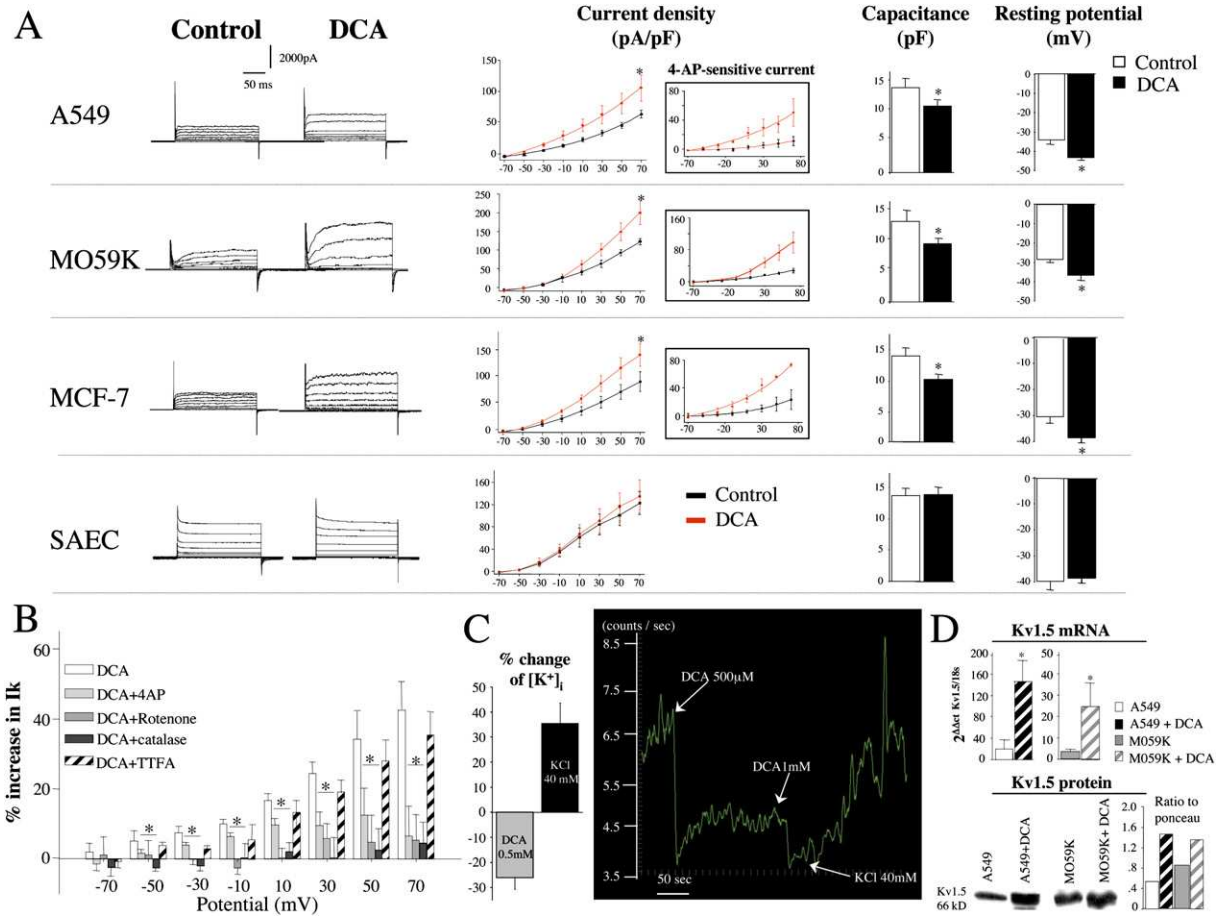

Figure 4. DCA Activates a Kv Current and Induces the Expression of Kv1.5 in Cancer, but Not Healthy, Cells

(A) Forty-eight hours of DCA (0.5 mM) increases K^+ current density (current amplitude/cell capacitance, pA/pF) in all cancer cell lines (A549, MO59K, and MCF-7) but does not affect noncancerous SAEC. On the left, original traces representing the K^+ current in both untreated and DCA-treated cells are shown. The increase in K^+ current density is mainly due to an increase in Kv current, as most of the increased current is 4-aminopyridine sensitive. Current subtraction was performed and the DCA-induced Kv current is shown in the insets. DCA treatment also causes a significant decrease in membrane capacitance and an increase in the plasma-membrane resting potential (*$p < 0.05$ versus control).

(B) The mechanism by which DCA increases K^+ current was assessed by exposing cancer (A549) cells to DCA (0.5 mM) acutely (5–10 min). The effects of DCA on K^+ current were blocked by 4-aminopyridine (5 mM), catalase (10,000 units, intracellularly via pipette), and rotenone (5 μM), whereas a specific blocker of complex II (TTFA, 1 μM) did not alter the DCA effects (*$p < 0.05$ versus control).

(C) DCA decreases $[K^+]_i$ and this is inhibited when the K^+ gradient is diminished by adding extracellular KCl.

(D) DCA-treated cells (48 hr) have increased Kv1.5 mRNA and protein, compared to the untreated cells (*$p < 0.05$ versus untreated cells).

(TTFA; an inhibitor of complex II of the ETC) (Figure 4B, n = 5). It was also not blocked by the human *ether-a-go-go*-related gene (HERG) inhibitor E4031 (50 nM) (Wang et al., 2002) (not shown). The activation of Kv channels by DCA resulted in a decrease in intracellular K^+, due to efflux of K^+ down its concentration gradient. When this gradient was diminished by the addition of KCl, the intracellular K^+-lowering effects of DCA were inhibited (Figure 4C, n = 20).

DCA Decreases $[Ca^{2+}]_i$ and Increases Kv1.5 Expression via Inhibition of NFAT1

We have recently shown that DCA increases the expression of Kv1.5 in PASMC (McMurtry et al., 2004). Only one study has linked Kv1.5 with cancer: Kv1.5 expression (but not other Kv channels) correlates with tumor grade in human gliomas, that is, the higher the grade, the lower the Kv1.5 (Preussat et al., 2003). We used quantitative real-time polymerase chain reaction (n = 5) and immunoblots and showed that Kv1.5 is significantly increased in DCA-treated A549 cancer cells (Figure 4D), in contrast to Kir2.1, a K^+ channel from a different family (not shown).

To study whether Kv1.5 expression correlates with human tumor grade, we used archived tumors from a cohort of 30 consecutive patients with non-small-cell lung cancer. We measured both Kv1.5 and survivin expression in each tumor sample and correlated their levels with histologic tumor grade by blinded readers. Survivin, a marker of resistance to apoptosis and tumor aggressiveness, has recently been shown to regulate mitochondria-dependent

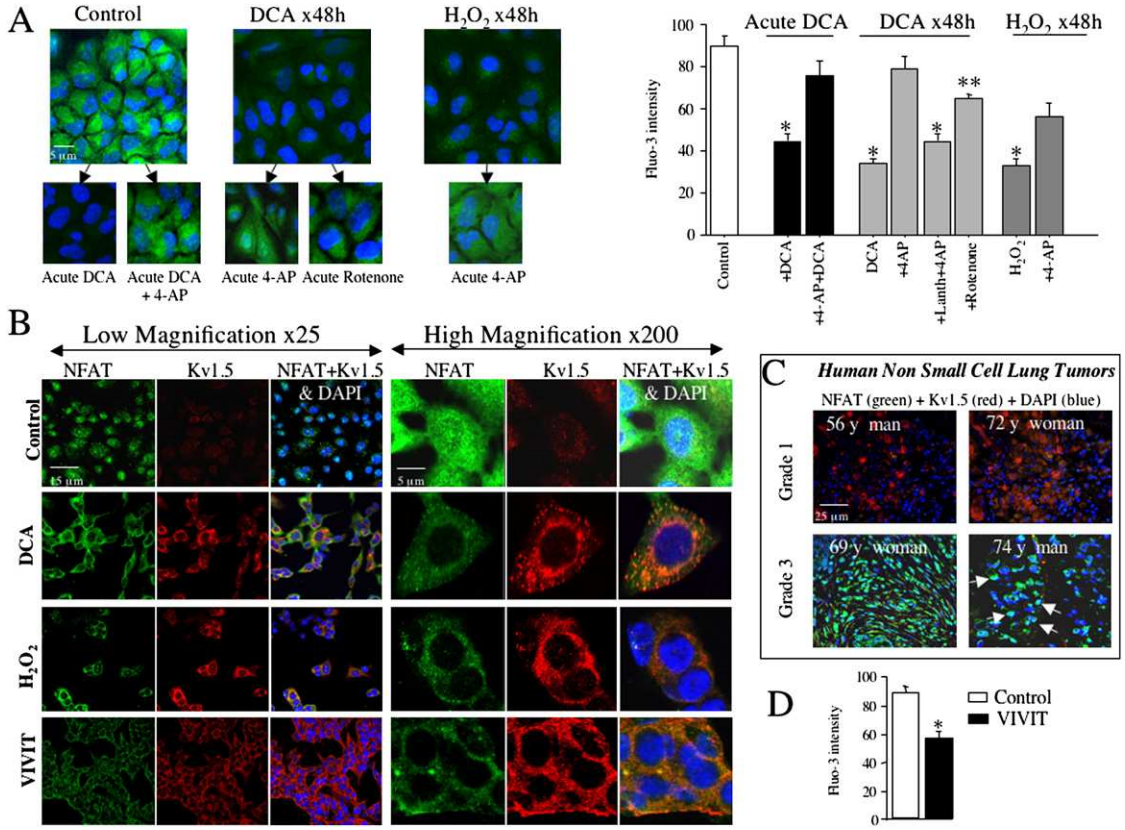

Figure 5. DCA Upregulates Kv1.5 by Decreasing $[Ca^{2+}]_i$ and Inhibiting the Ca^{2+}-Dependent Transcription Factor NFAT1

(A) Free cytosolic calcium ($[Ca^{2+}]_i$) concentration was measured using FLUO-3. Untreated A549 cells have higher $[Ca^{2+}]_i$ than both DCA- and t-butyryl-H_2O_2-treated cells. The decrease in $[Ca^{2+}]_i$ by DCA and H_2O_2 is inhibited by 4-aminopyridine (5 mM), suggesting that it involves the opening of Kv channels. It is also blocked by rotenone (5 μM), suggesting that it involves ROS produced in complex I. Lanthanum (10 μM) prevents the effects of 4-aminopyridine (*$p < 0.01$, **$p < 0.05$, compared to untreated controls).

(B) Confocal imaging and triple-staining of A549 cells showed that NFAT1 (green) is activated, as it is mainly localized in the nuclei (stained blue by DAPI) of most of the untreated cells. These cells have a very low level of Kv1.5 expression (red). Both DCA and H_2O_2 block the activation of NFAT1, as it is mainly localized in the cytoplasm; the cells with the cytoplasmic NFAT1 have proportionately increased Kv1.5 expression. The NFAT inhibitor VIVIT (4 μM) displaces NFAT1 from the nucleus and causes a significant upregulation of Kv1.5.

(C) Representative clinical specimens of non-small-cell lung cancer, showing that NFAT1 activation is associated with decreased Kv1.5 expression and higher histologic grade. Within each sample, the lowest Kv1.5 expression is seen in cells with activated NFAT1 (arrows).

(D) By upregulating Kv1.5, VIVIT decreases $[Ca^{2+}]_i$, suggesting that the reason for increased $[Ca^{2+}]_i$ levels in the cancer cells involves a downregulation of Kv1.5.

*$p < 0.05$ versus control.

apoptosis in both cancer (Dohi et al., 2004) and vascular tissues (McMurtry et al., 2005). Survivin correlated positively with tumor grade while Kv1.5 correlated negatively (the higher the Kv1.5, the lower the grade), and no differences in the expression of Kir2.1 were seen (Figure S2).

Because NFAT (nuclear factor of activated T lymphocytes) inhibits both apoptosis (Pu et al., 2003) and the expression of Kv1.5 in myocardial cells (Rossow et al., 2004), we speculated that this could also occur in cancer. Increases in $[Ca^{2+}]_i$ activate calcineurin, which dephosphorylates NFAT, allowing its translocation to the nucleus where it regulates gene transcription (Macian, 2005). We hypothesized that the DCA-induced activation of Kv1.5 leads to plasmalemmal hyperpolarization, inhibiting voltage-gated Ca^{2+} channels (which are active even in nonexcitable cells; Dietl et al., 1995), decreasing $[Ca^{2+}]_i$, thereby inhibiting NFAT and enhancing Kv1.5 expression (Figure 1).

As predicted, DCA-treated A549 cells have lower $[Ca^{2+}]_i$ compared to untreated cells (Figure 5A). The decrease in $[Ca^{2+}]_i$ occurs within 5 min and is sustained after 48 hr of DCA exposure. At both time points, DCA's effects on $[Ca^{2+}]_i$ are inhibited by 4-aminopyridine and rotenone and are mimicked by t-butyryl-H_2O_2, suggesting that they involve opening of Kv channels by complex I-derived H_2O_2 ($n \sim 20$ plates/group). The 4-aminopyridine-induced increase in $[Ca^{2+}]_i$ in the DCA-treated cells is inhibited by lanthanum ($n = 6$), a blocker of Ca^{2+} entry into the cell (Figure 5A), confirming an operative voltage-dependent pathway of Ca^{2+} entry.

NFAT1 activation (defined by its translocation to the nucleus) is evident in the majority of untreated A549

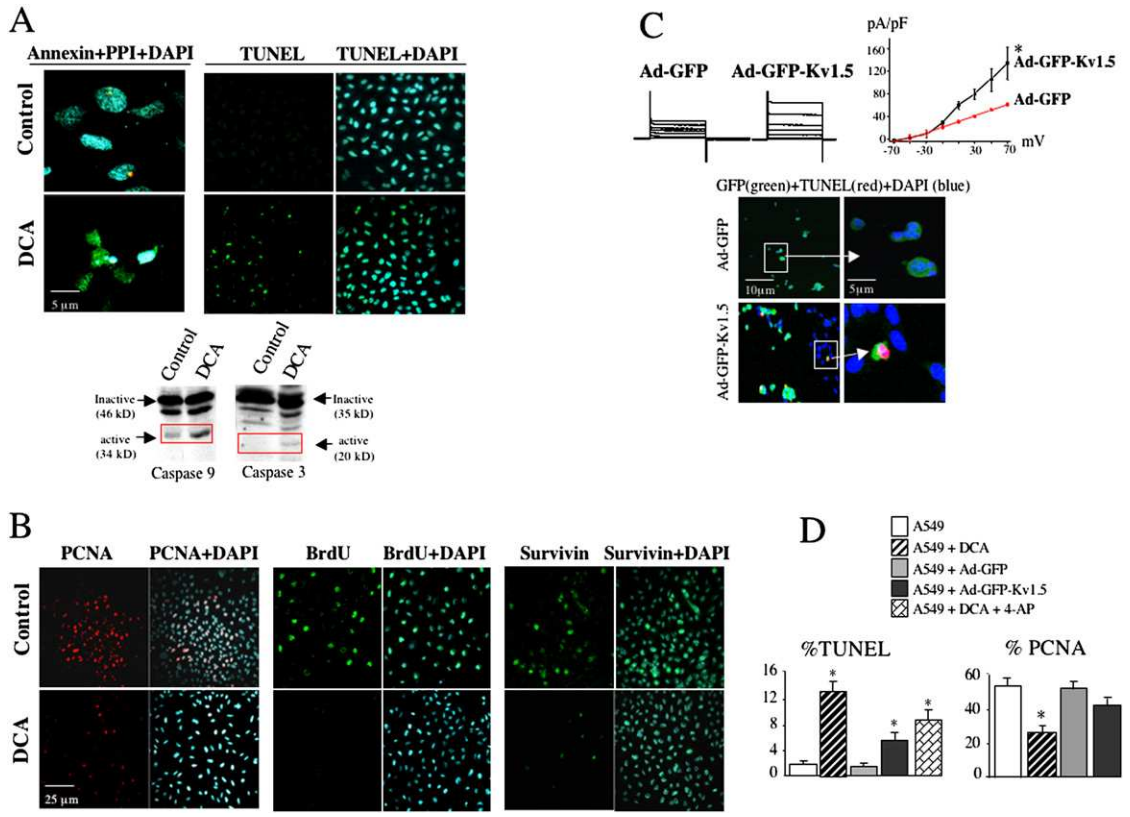

Figure 6. DCA Induces Apoptosis and Decreases Proliferation in Cancer Cells by a Dual Mechanism Involving Mitochondria and Upregulation of Kv1.5

(A) DCA increases apoptosis in A549 cells as shown by the expression of annexin and the increased % of TUNEL-positive cells (mean data in [D]), compared to the untreated controls. The absence of propidium iodide (PPI) staining in the annexin-positive cells suggests that the cells were apoptotic and not necrotic. DCA activates both caspase 3 and 9, as immunoblots reveal an active band for both caspases.

(B) DCA treatment decreases cell proliferation, measured by PCNA (mean data in [D]) and BrdU. DCA also decreases the expression of survivin.

(C and D) Kv1.5 gene transfer using Ad-GFP-Kv1.5 adenovirus increases the K^+ current and induces apoptosis (for these experiments, TUNEL is red in GFP-positive cells), compared to the cells infected with Ad-GFP (C). However, this exogenous gene transfer of human Kv1.5 causes less apoptosis and smaller inhibition of proliferation compared to the DCA-treated cells (D), despite a larger increase in the outward K^+ current (compare with Figure 4). 4-aminopyridine decreases DCA-induced apoptosis by ~32% (also see Figure S4).

*$p < 0.05$ versus controls.

cells, and in these cells Kv1.5 expression is low (Figure 5B). In contrast, in DCA-treated cells, NFAT1 is mostly cytoplasmic and Kv1.5 expression is proportionately increased. As with Ik (Figure 4B) and $[Ca^{2+}]_i$ (Figure 5A), the effects of DCA on NFAT1 were mimicked by t-butyryl-H_2O_2 (Figure 5B). We then treated A549 cells with VIVIT, a competing peptide that selectively blocks NFAT-regulated mechanisms due to its ability to block calcineurin docking on NFAT, preventing its activation without inhibiting calcineurin's catalytic site (Aramburu et al., 1999). The VIVIT-treated cells show displacement of NFAT1 from the nucleus and increased Kv1.5 expression (Figure 5B). The same was true for cells treated with cyclosporine, a nonspecific inhibitor of calcineurin (Figure S3A).

In human non-small-cell lung tumors costained with anti-Kv1.5, anti-NFAT1, and 4′,6-diamidino-2-phenylindole (DAPI), low-grade histology was associated with high Kv1.5 expression and low NFAT1 expression, most of which was cytoplasmic; the reverse pattern was seen in high-grade tumors (Figure 5C).

The effects of NFAT1 might be potentiated by a positive feedback loop: low Kv1.5 → depolarized plasma membrane → Ca^{2+} influx → high $[Ca^{2+}]_i$ → activated NFAT → low Kv1.5. NFAT inhibition effectively breaks this loop because VIVIT decreases $[Ca^{2+}]_i$ (n = 5 plates/group, Figure 5D).

DCA Induces Mitochondria-Dependent Apoptosis and Decreases Proliferation In Vitro

DCA increases annexin expression, causes a ~6-fold increase in the percentage of TUNEL-positive nuclei, and activates both caspase 3 and 9 in A549 cells (Figures 6A and 6D). Eliminating highly proliferative cells by the induction of apoptosis, and by decreasing $[Ca^{2+}]_i$ levels, DCA decreases indices of proliferation (Figures 6B and 6D) including BrdU incorporation and expression of proliferating cell nuclear antigen (PCNA).

In addition, DCA decreases the expression of survivin (Figure 6B).

DCA-induced apoptosis proceeds by two pathways, one in the mitochondria, where depolarization activates mitochondria-dependent apoptosis, and the other at the plasmalemmal level, where activation/upregulation of Kv1.5 channels decreases $[K^+]_i$, activating caspases. To determine the relative importance of the two mechanisms, we compared the apoptosis induced by DCA to the apoptosis induced by a primary increase in Kv1.5 expression, using adenoviral gene transfer (Figures 6C and 6D). Compared to the adenovirus carrying green fluorescent protein (GFP) only, the adenovirus carrying GFP and cloned human Kv1.5 (Pozeg et al., 2003) significantly increased the percentage of TUNEL-positive cells. However, although the increase in Ik achieved with the gene transfer was higher than the increase achieved by DCA (Figure 6C; compare with Figure 4A), the increase in apoptosis achieved by the gene transfer was significantly less than that achieved by DCA (Figure 6D). We then measured the DCA-induced apoptosis in the presence of 4-aminopyridine (5 mM), a blocker of the whole Kv family. In addition to the A549 cells we also studied glioblastoma, an excitable cell type in which Kv channels might be more important in apoptosis regulation compared to the epithelial A549 cells. In the presence of 4-aminopyridine, DCA induced 68% of the apoptosis (% TUNEL-positive cells) induced by DCA alone (Figure 6D). Similarly, in glioblastoma cells, DCA + 4-aminopyridine induced 62% of the apoptosis induced by DCA alone (Figure S4). Moreover, 4-aminopyridine did not limit DCA's ability to cause efflux of cytochrome *c* from mitochondria, initiating mitochondria-based apoptosis (Figure S4). These data underlie the preponderant importance of the mitochondrial component of DCA's proapoptotic actions.

That NFAT1 is a distal mediator in DCA's anticancer effects was supported by the fact that VIVIT increased apoptosis and decreased proliferation in a manner similar to DCA (Figure S3B). For imaging studies, we studied four random fields per slide for ~30 slides/group, and for patch clamping, 6–8 cells/group.

Molecular Inhibition of PDK2 Mimics DCA

To confirm that inhibition of PDK is the major mechanism for the effects of DCA, we determined whether molecular inhibition of PDK2 by siRNA mimics DCA. We chose PDK2 because it is the only ubiquitously expressed isoenzyme; PDK1 and 3 are restricted in the heart and testis, respectively, and PDK4 is mostly expressed in skeletal muscle and heart. PDK2 is the most active of all and also has the lowest Ki for DCA (0.2 mM) (Bowker-Kinley et al., 1998). siRNA for PDK2 inhibited the expression of PDK2 in a dose-dependent manner, inhibiting mRNA up to 80% and protein expression (measured by both immunoblots and immunohistochemistry) by ~70% (Figure S5). We tested three commercially available PDK2 siRNAs, which all inhibited the gene in a similar manner. Scrambled siRNA for PDK2 as well as siRNA for PDK1 did not decrease PDK2 expression (Figure S5). Whereas the scrambled siRNA had no effect on A549 cells, PDK2 siRNA decreased $\Delta\Psi m$ and increased mitochondrial ROS in a manner identical to DCA (Figures 7A and 7B, n ~ 20 plates/group). DCA added to siRNA-treated cells had no additional effects (data not shown). Inhibition of PDK2 by siRNA also increased apoptosis and decreased proliferation in cancer cells (Figure 7C, n ~ 30 plates/group). To further prove that DCA activates PDH by inhibiting PDK, we immunoprecipitated PDH and showed that DCA increased the nonphosphorylated fraction (i.e., active) of the catalytic subunit (E1α) (Figure 7D).

DCA in the Drinking Water Induces Apoptosis and Decreases Tumor Growth In Vivo

We studied nude athymic rats implanted subcutaneously with 3×10^6 A549 cells. The rats had free access to water with or without DCA (75 mg/l). In the first set of experiments (protocol a), 21 animals were divided into three groups: untreated controls (n = 5), DCA-prevention rats (n = 8), which received DCA just after cell injection for 5 weeks, and DCA-reversal rats (n = 8), which received DCA 2 weeks post-cell injection for 3 more weeks. The untreated rats rapidly developed tumors with a constant exponential tumor growth (Figure 8A). Both DCA-treated groups had a significant decrease in tumor size, measured by tumor weight at sacrifice and maximal diameter using calipers; in some rats, in vivo magnetic resonance imaging allowed us to visualize the tumors in vivo and calculate their volume. The decrease in tumor growth by DCA was associated with an increase in apoptosis (TUNEL) and a decrease in proliferation (PCNA) (Figure 8B). There was an inverse correlation between apoptosis and tumor size in the treated rats (Figure 8B). Kv1.5 was upregulated and survivin was downregulated in the DCA-treated rats (Figure 8C), confirming our in vitro data (Figures 4 and 6).

In a second set of experiments (protocol b), we studied whether the effects of DCA were sustained for longer periods of time and whether DCA would have a similar effect in more advanced tumors. We followed three groups of rats (n = 6/group) for 12 weeks: an untreated control group, a prevention group (rats given DCA at the time of tumor cell injection), and a reversal group where rats were given DCA at week 10 for 2 weeks. As in protocol a, at all times rats in the prevention group had significantly smaller tumors compared to the untreated controls; DCA at week 10 inhibited tumor growth immediately, with a significant decrease even after 1 week of treatment. DCA therapy did not have any toxic effects, as measured by several blood tests (Figure 8D; also see McMurtry et al., 2004).

DISCUSSION

Here we show that a metabolic-electrical remodeling (hyperpolarized mitochondria, downregulated Kv channels) regulates the apoptosis resistance that characterizes multiple human cancers. DCA, a small molecule that targets mitochondria, reverses this remodeling, inducing

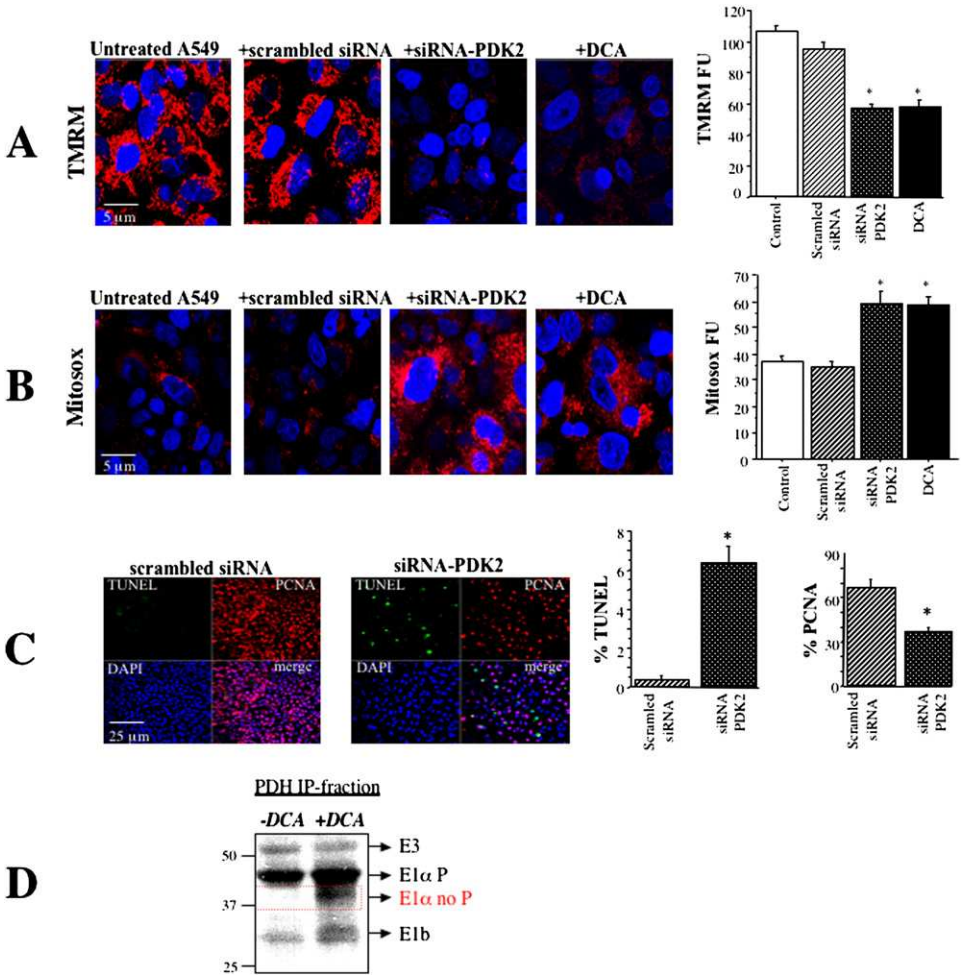

Figure 7. DCA Activates PDH by Inhibiting PDK2; Molecular Inhibition of PDK2 by siRNA Mimics DCA

(A) Effective inhibition of PDK2 expression by siRNA (see Figure S1) depolarizes A549 mitochondria in a manner similar to DCA, whereas scrambled siRNA has no effect.

(B) siRNA inhibition of PDK2 also mimics DCA in increasing mitochondria-derived ROS, as measured with the fluorescent dye mitosox.

(C) siRNA inhibition of PDK2 increases apoptosis (% TUNEL-positive cells), similar to DCA.

(D) Human PDH was immunoprecipitated from A549 cells and treated with a cocktail of monoclonal antibodies against several PDH subunits. In the untreated cancer cells, the E1α subunit (i.e., the catalytic subunit) is all in the phosphorylated form, indicating maximal inhibition of PDH by PDK. In the DCA-treated cells, the nonphosphorylated fraction of the E1α subunit is significantly increased, indicating an increase in the activity of PDH.

*$p < 0.05$ versus controls.

apoptosis and decreasing cancer growth in vitro and in vivo. These beneficial effects occur without affecting noncancerous cells or eliciting systemic toxicity. DCA treatment significantly increases glucose oxidation (which only occurs in functional mitochondria), indicating that the well-recognized, metabolic cancer signature (aerobic glycolysis) is reversible, rather than a consequence of permanent mitochondrial damage. DCA exerts its beneficial effects by two pathways, both of which induce apoptosis: first, by mitochondrial depolarization and efflux of proapoptotic mediators, and second, by an increase in Kv channel expression/function. DCA increases Kv channel expression by inhibiting NFAT1, a calcium-sensitive transcription factor that regulates cell-differentiation programs in many cell types but which has previously been unexplored in cancer. The mitochondria-NFAT-Kv pathway in cancer offers several new candidate targets for proapoptotic therapy that would be predicted to have high therapeutic selectivity.

Glycolysis and Cancer: Not Just an Epiphenomenon

It is now well accepted that most cancers have a glycolytic phenotype. Warburg suggested, but did not prove, that this was due to "abnormal mitochondria" (Warburg, 1930); that is, cancer cells are forced to use inefficient, nonmitochondrial means of generating ATP. Our data suggest that this apparent mitochondrial "dysfunction" is in fact reversible. Oxidative metabolism in cancer could be actively suppressed; the resultant shift to glycolysis may lead to apoptosis resistance (Plas and Thompson, 2002), offering

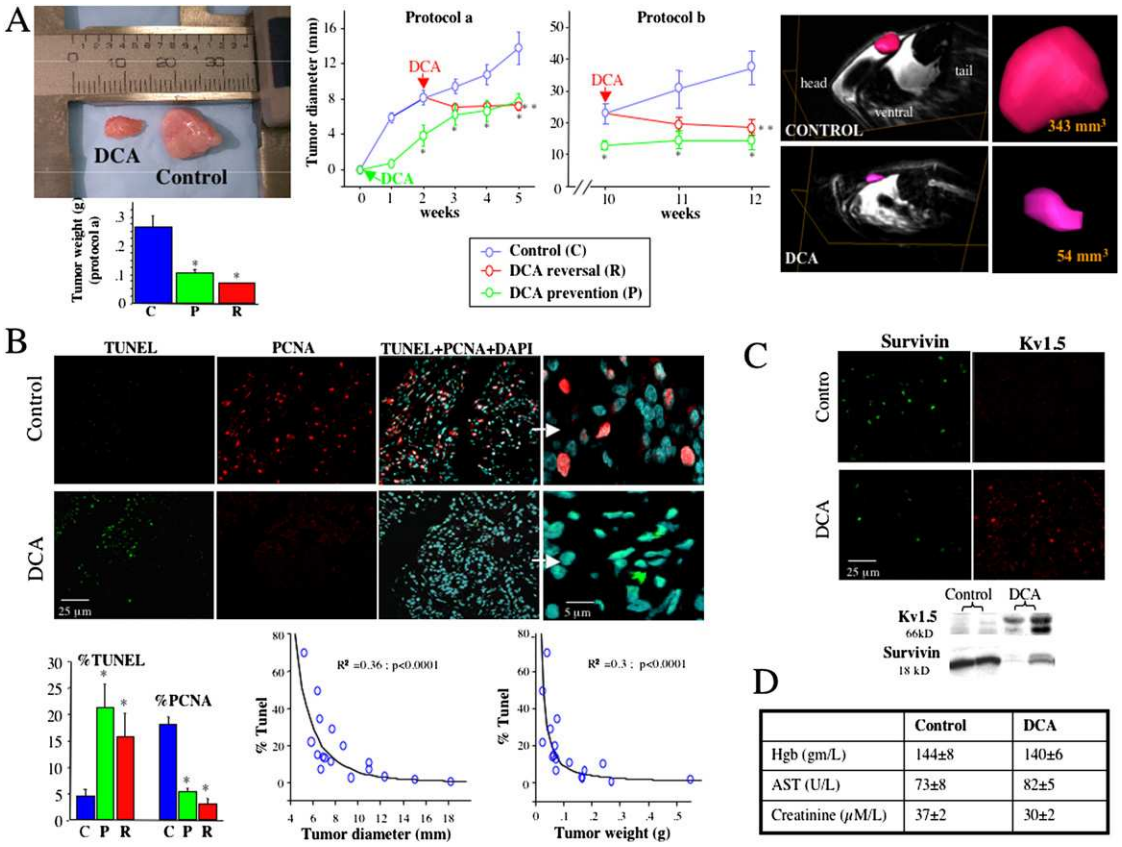

Figure 8. Decreased Tumor Size in DCA-Treated Nude Rats Is Due to an Increase in Apoptosis and Decrease in Cell Proliferation

(A) Injection of A549 cells into the flank of nude rats results in the development of measurable tumors within 1 week. DCA-treated rats in both the prevention and reversal groups of protocols a and b (see Results) have smaller tumors. The size of the tumors was assessed by weight, calipers, or magnetic resonance imaging in vivo and at the time of euthanasia, as shown.

(B) DCA-treated rats had smaller tumors due to a significant increase in apoptosis (TUNEL) and a decrease in proliferation (PCNA), as shown by triple-staining. A significant correlation was observed between % TUNEL and both tumor diameter and weight (the higher the % of TUNEL-positive cells, the smaller the tumor).

(C) In agreement with our in vitro data, DCA increases Kv1.5 and decreases survivin expression, as shown by both immunohistochemistry and immunoblotting.

(D) DCA-treated rats did not have any sign of liver (AST), kidney (creatinine), or blood (hemoglobin) toxicity.

*$p < 0.05$ versus untreated controls.

a survival advantage in the transformed cells (Gatenby and Gillies, 2004). This suggests that a novel way to reverse apoptosis resistance might be to undo this metabolic/mitochondrial remodeling. We show that the glycolytic phenotype in cancer is easily altered by promoting oxidative phosphorylation (Figure 2C). This is associated with mitochondrial depolarization, which facilitates apoptosis and inhibits tumor growth. All the human cancer cell lines studied had more negative $\Delta\Psi m$ compared to several noncancerous cell lines (Figure 2A), suggesting that this might be a hallmark of malignancy. Although apoptosis is not always associated with mitochondrial depolarization, our data are in agreement with the observation that cationic lipophilic drugs preferentially accumulate to tumor mitochondria (Don and Hogg, 2004). In addition, the positively charged rhodamine-based dyes (like TMRM) have been tried as "carriers" for selective delivery of drugs in cancer. More than 200 carcinomas were screened and were shown to accumulate rhodamine much more than non-carcinoma cells; these findings were first reviewed in 1988 (Chen, 1988), and although the mechanism was not clear then, it likely reflects the more negative $\Delta\Psi m$ of cancer compared to noncancerous cells. Our work directly shows that this relative increase in $\Delta\Psi m$ is associated with increased resistance to apoptosis, and its "normalization" increases apoptosis and decreases cancer growth. Furthermore, it has just been shown that $\Delta\Psi m$ of colon cancer cells predicts the aggressiveness of the tumor cells, that is, the more hyperpolarized the $\Delta\Psi m$, the more aggressive and metastatic the tumor (Heerdt et al., 2005), in agreement with our proposal. Studying $\Delta\Psi m$ in fresh tumor specimens might be a convenient means to predict resistance to proapoptotic chemotherapies, with important implications in clinical decision making.

How Does DCA Alter Metabolism, Depolarize Mitochondria, and Initiate Apoptosis?

The shift in the metabolism of pyruvate away from lactate and toward acetyl-CoA and the Krebs cycle (Figures 2C and 2D), caused by DCA or molecular inhibition of PDK2 (Figure 7), increases the intramitochondrial production of the electron-donor NADH (Figure 3C), a substrate of the ETC complex I, leading to increased complex I-based ROS production (Figures 3B and 7B) (Kushnareva et al., 2002). A sustained increase in the ROS production can cause oxidative damage in the ETC, particularly complex I. This megacomplex is the most sensitive of all ETC complexes to ROS damage because it is by far the largest (46 subunits), and has at least nine ROS-sensitive iron-sulfur centers and seven mitochondrial DNA-encoded subunits (Brandt, 2006), which are very susceptible to oxidative damage. The ROS-induced complex-I dysfunction can limit the efflux of H^+, decreasing $\Delta\Psi m$. Upon sustained and significant decrease in $\Delta\Psi m$, the voltage-sensitive MTP opens (Zamzami and Kroemer, 2001), allowing the efflux of many proapoptotic factors and the initiation of apoptosis (Figures 3A, 6, and 8B). This further increases the production of mitochondrial ROS, likely reinforcing a positive feedback loop enhancing apoptosis (Zamzami and Kroemer, 2001).

This "complex I-centered" proposed mechanism has a precedent in congenital mitochondrial syndromes and neurodegenerative diseases. Patients with congenital complex-I deficiency have decreased $\Delta\Psi m$ and increased ROS production (Pitkanen and Robinson, 1996). Inhibition of complex I in cell lines is associated with decreased $\Delta\Psi m$ and increased ROS production in a dose-dependent manner, that is, the higher the percent complex-I inhibition, the higher the ROS and the lower the $\Delta\Psi m$ (Barrientos and Moraes, 1999). A similar mechanism where dose-dependent inhibition of complex I leads to dose-dependent efflux of cytochrome *c* and apoptosis (Clayton et al., 2005) is proposed in the pathogenesis of neurodegenerative diseases such as Parkinson's, where complex-I dysfunction and ROS-mediated oxidative damage are well described (Bao et al., 2005; Schon and Manfredi, 2003).

Inhibition of VDAC limited the DCA-induced decrease in $\Delta\Psi m$ (Figure 3D). VDAC (along with the adenine nucleotide translocase) is involved in the translocation of ADP (a substrate for the F1F0-ATPase) from the cytoplasm into the mitochondria. Inhibition of the VDAC would thus inhibit the function of the F1F0-ATPase, which would lead to accumulation of H^+ in the intermembrane mitochondrial space, promoting hyperpolarization of the $\Delta\Psi m$, thus limiting the depolarizing effects of DCA. This is supported by findings from Thompson's group (Vander Heiden et al., 1999), although the role of VDAC in the regulation of $\Delta\Psi m$ and initiation of apoptosis remains controversial (Shimizu et al., 1999) (reviewed in Granville and Gottlieb, 2003), and some of these mechanisms might only be relevant to specific experimental conditions, such as growth-factor withdrawal (Vander Heiden et al., 1999). An additional intriguing possibility is that, because DCA is itself an anion (see structure in Figure 1), it likely enters the mitochondria via the VDAC, explaining, at least in part, why its inhibition limits the effects of DCA on $\Delta\Psi m$.

Unexpectedly, but consistent with its therapeutic benefit, DCA decreased the expression of survivin, an inhibitor of apoptosis, both in vitro and in vivo (Figures 6 and 8). Survivin has recently emerged as a major antiapoptotic oncoprotein. The mechanism by which survivin is downregulated is unclear. Recent observations describing the direct involvement of a mitochondrial survivin pool in the suppression of apoptosis suggest that survivin might participate in the mitochondrial remodeling of cancer (Dohi et al., 2004; McMurtry et al., 2005).

A Mitochondria-NFAT-Kv Channel Axis in Cancer Is Normalized by DCA, Contributing to the Proapoptotic and Antiproliferative Effects of DCA

The apoptosis resistance in cancer likely involves multiple mechanisms. The current findings highlight the contribution of Kv channel inhibition/downregulation, due to impaired mitochondrial signaling, to this resistance. Closing of K^+ channels or decreasing their expression results in an increase in $[K^+]_i$ which increases the tonic inhibition that cytosolic K^+ exerts on caspases. Kv1.5 gene transfer directly activated apoptosis in A549 cells (Figures 6C and 6D). Functional inhibition of all Kv channels by 4-aminopyridine limited the DCA-induced apoptosis by ~32% in A549 cells and by ~38% in glioblastoma cells (Figure 6D; Figure S4), suggesting that although the majority of apoptosis in DCA-treated cells is a direct result of efflux of proapoptotic mediators from cancer cells, the secondary effects on Kv channels also play an important role.

The precise role of K^+ channels in cancer remains unclear, and although K^+ channel opening promotes apoptosis in several tumors, the opposite result has also been noted (reviewed in Wang, 2004). Perhaps this relates to the type of tumor or the well-known diversity of K^+ channel families. Specific K^+ channels are now emerging as important regulators of apoptosis in different cell types. For example, HERG, a Kv channel, mediates H_2O_2-dependent apoptosis in various cancer cell lines (i.e., low HERG expression reduces apoptosis and enhances proliferation) (Wang et al., 2002). Kv1.5 regulates apoptosis in PASMC (Remillard and Yuan, 2004) and is downregulated in the proliferative and apoptosis-resistant vascular media in pulmonary hypertension (McMurtry et al., 2004, 2005; Pozeg et al., 2003). A teleological advantage of Kv1.5 as a regulator of apoptosis in cancer, and a factor which focused our attention on this channel, is its very short turnover time, less than 8 hr from transcription to functional expression (Levitan et al., 1995).

We show that cancer cells are deficient in ETC complex I-based production of H_2O_2, a Kv1.5 channel opener (Figure 3B). Perhaps more importantly, Kv1.5 is downregulated in cancer cell lines (Figure 4D), and Kv1.5 expression correlates inversely with histologic grade in a cohort of patients with non-small-cell lung cancer (more aggressive tumors have less Kv1.5) (Figure S2). We have identified NFAT1 as an important transcription factor responsible for this Kv1.5 downregulation (more aggressive cancers have more activated NFAT1) (Figure 5C).

The cellular environment in cancer is favorable for NFAT activation. A549 cells have increased $[Ca^{2+}]_i$ (Figure 5A), a direct activator of calcineurin and thus NFAT (Macian, 2005). This increase in $[Ca^{2+}]_i$ is, at least in part, due to the increased Ca^{2+} influx that results from the Kv channel deficiency (Figure 4). In addition, calcineurin is inhibited by increased ROS levels (Namgaladze et al., 2005); thus, the low mitochondrial ROS in cancer (Figures 3B and 7B) promote NFAT activation. Furthermore, the acidotic environment in cancer (due to aerobic glycolysis) (Figure 2E) would further promote NFAT activation (Komarova et al., 2005). It is remarkable that all of these mechanisms are reversed by DCA, which increases ROS, increases pH, and decreases $[Ca^{2+}]_i$, explaining its impressive effects on NFAT (Figure 5B). The upregulation of Kv1.5 by a drug that directly affects mitochondrial function suggests the presence of the mitochondria-NFAT-Kv1.5 axis, which is suppressed in cancer. Our work suggests that potential effects on Kv channels should be considered in cancer therapies targeting the mitochondria.

Metabolic Modulation in Cancer by DCA: Possibility of Prompt Translation to Clinical Oncology

Our work suggests that metabolic modulators could be beneficial in human cancer, either alone or in combination with traditional chemotherapies, as apoptosis sensitizers. By targeting a fundamental and unique property of cancer cells, this approach may combine efficacy and selectivity. DCA (in clinically relevant doses; Stacpoole et al., 2006) was effective in preventing and inhibiting tumor growth in established tumors both early (week 2) and late (week 10) in their development (Figure 8A). DCA's effects in the reversal protocols were immediate, with significant effects even after 1 week of treatment. The relative specificity of DCA to target a metabolic (mitochondria) and electric (K^+ channels) remodeling was confirmed by microarray experiments, where pathway analysis revealed a short list of altered mitochondrial apoptosis cell cycle and ion channel genes (Supplemental Results; Figure S6).

A very attractive property of DCA is its selectivity, evident by the lack of any systemic toxicity in this (Figure 8D) and other recent animal (McMurtry et al., 2004) and human studies (Stacpoole et al., 2006). DCA's ability to "restore" $\Delta\Psi m$ might explain why it is effective preferentially in cells that have very high $\Delta\Psi m$, such as cancer cells, but has no effects in normal cells (epithelial, fibroblasts, or PASMC). Preferential expression of PDK might also contribute to its selectivity. In a recent study of non-small-cell lung cancer specimens, cancer cells had increased PDK2 and decreased PDH expression (compatible with a glycolytic phenotype) compared to neighboring nonmalignant cells (Koukourakis et al., 2005).

The small size of DCA results in excellent tissue penetration after oral intake, including the central nervous system (Stacpoole et al., 2003), relevant to the difficult-to-treat glioblastoma, one of the tumors that we studied in vitro. In addition, DCA decreases tumor lactic-acid production and increases intracellular pH (Figure 2E); future studies need to address the hypothesis that this will decrease tumor invasiveness and metastatic potential (Gatenby and Gillies, 2004).

Our work identifies the mitochondria-NFAT-Kv channel axis and PDK as critical components of the metabolic-electrical remodeling that characterizes many human cancers and offers a tantalizing suggestion that DCA may have selective anticancer efficacy in patients. The very recent report of the first randomized long-term clinical trial of oral DCA in children with congenital lactic acidosis (at doses similar to those used in our in vivo experiments) showing that DCA was well tolerated and safe (Stacpoole et al., 2006) suggests a potentially easy translation of our work to clinical oncology.

EXPERIMENTAL PROCEDURES

The use of human tissues was approved by the University of Alberta Human Ethics Committee, and all experiments with rodents were approved by the University of Alberta Animal Ethics Committee (Health Sciences Laboratory Animal Services).

Confocal Microscopy

Imaging was performed using a Zeiss LSM 510 multiphoton confocal microscope (Carl Zeiss Canada, Toronto, ON) and multiple-staining techniques, as previously described (McMurtry et al., 2004, 2005). For details, see Supplemental Data.

Metabolic Studies

A549 cells were grown to confluency in T-175 flasks and rates of glycolysis, fatty acid oxidation, and glucose oxidation were measured as previously described (Saddik et al., 1993) in the presence or absence of DCA (0.5 mM, 48 hr); also see Supplemental Data.

Ca^{2+} Measurements

Intracellular free Ca^{2+} concentration ($[Ca^{2+}]_i$) was studied in live A549 cancer cells using FLUO-3AM (Invitrogen-Molecular Probes Canada, Burlington, ON). Cells were loaded with FLUO-3AM (5 μmol/l) for 45 min (37°C) in serum-free medium and washed for 30 min in PBS (37°C) to allow cleavage of the acetoxymethyl esters. In association with FLUO-3, Hoechst (1.0 μmol/l) nuclear staining was applied for 10 min (Molecular Probes). Fluorescence was measured at 505–535 nm with excitation at 488 nm.

H_2O_2 Measurements

Cancer cells were propagated on LabTek multiwell slides (Nalge Nunc, Rochester, NY, USA; VWR, Mississauga, ON, Canada) until confluent. Monolayers were preincubated with DCA in the presence or absence of 5 μM rotenone (Sigma-Aldrich Canada, Oakville, ON) for 1 hr. Production of H_2O_2 was measured by the AmplexRed assay (Molecular Probes). Fluorescence was measured at 590 nm with excitation at 530 nm, and H_2O_2 levels were determined by reference to a standard curve, as previously described (McMurtry et al., 2004).

Electrophysiology

With standard whole-cell patch-clamping techniques, cells were voltage clamped at a holding potential of −70 mV and currents were evoked by 200 ms test pulses from −70 to +70 mV with 20 mV steps, filtered at 1 kHz, and sampled at 2–4 kHz, as previously described (McMurtry et al., 2004, 2005).

Immunoblotting and Quantitative Real-Time Polymerase Chain Reaction

For details, antibodies, and primers, see Supplemental Data.

Kv1.5 Gene Transfer

A549 cells were infected with replication-deficient serotype-5 adenovirus encoding genes for GFP and cloned human Kv1.5 (both under

cytomegalovirus [CMV] promoters) as previously described (McMurtry et al., 2005; Pozeg et al., 2003). We achieved 80% infection rates, and infected cells were selected on the basis of their green fluorescence.

In Vivo Tumorigenicity Assays

A cell suspension of A549 cells in PBS (3×10^6 cells per injection) was injected subcutaneously into nude athymic rats. Rats were divided into control (no treatment), prevention, and reversal groups, and two protocols were followed. In protocol a, rats were followed for 5 weeks: the prevention group was treated for 5 weeks and the reversal group for 3 (weeks 3–5). In protocol b, rats were followed for 12 weeks, with the prevention group treated for 12 weeks and the reversal group from week 10 to week 12. In both protocols, DCA (0.075 g/l) was added to the drinking water. By measuring the amount of water consumed, we calculated and adjusted the concentration of DCA required to achieve a daily dose similar to that used clinically (50–100 mg/kg) (McMurtry et al., 2004; Stacpoole et al., 2006) Rats were observed weekly for the appearance of tumors at injection sites, and tumor size was measured every week with calipers in the three groups.

Intracellular K^+

Intracellular K^+ was studied ratiometrically, measuring the fluorescence of cells loaded with the acetoxymethyl ester form of PBFI (PBFI-AM; 5 μM; Molecular Probes). For details, see Supplemental Data.

Mitochondrial NADH

Mitochondria were isolated from both untreated and DCA-treated cells (500 μM, 48 hr), as previously described (Michelakis et al., 2002). Mitochondrial NADH ([NADH]m) was assessed using the methods described previously by Brandes and Bers (1996). The mitochondria were excited by light at 350 nm, and fluorescence was detected at 456 nm using a Photon Technology International Delta Scan 1 fluorescence spectrophotometer (London, ON, Canada). The fluorescence signal at 456 nm is known to predominantly arise from [NADH]m (Eng et al., 1989).

PDH Activity

PDH activity was assessed by measuring the amount of phosphorylated and unphosphorylated E1α subunits. Three milligrams of protein was isolated from untreated and DCA-treated cells. PDH subunits were isolated using the PDH complex immunocapture kit (MitoSciences, Eugene, OR, USA). The immunoprecipitated fraction was then used for immunoblotting using the human PDH subunits monoclonal antibody cocktail (MitoSciences).

siRNA Studies

A549 lung cancer cells were grown to 80% confluence in six-well culture dishes. The transfection agent siPORTamine (Ambion siRNA Transfection II kit 1631, Ambion, Austin, TX) was preincubated at room temperature for 10 min at a ratio of 1:12 in OptiMEM1 culture medium (Invitrogen-GIBCO Canada, 31985-070, Burlington, ON). This concentration of transfection agent had previously been demonstrated to result in at least 60% gene knockdown with less than 15% cell death (data not shown). The mixture was combined with 75, 37.5, or 18.7 nmol of scrambled versus silencer RNA for human PDK2 and PDK1 (Ambion) in an equivalent volume of OptiMEM1, and incubated for a further 10 min. The PDK2 silencer variants ID 264, 265, and 266 were also tested. The culture medium was aspirated from the cells, the transfection agent-RNA complex mixture was allowed to spread over the monolayer, and 1.5 ml of complete F12K was added. Plates were incubated at 37°C for 48 hr.

Cell Cultures

For sources of cell lines and culture media, see Supplemental Data.

Magnetic Resonance Imaging, DNA Microarrays, Intracellular pH Measurement, and Lactate Measurement

See Supplemental Data.

Statistics

Values are expressed as the mean ± SEM. Intergroup differences were assessed by Kruskal-Wallis or one-way ANOVA as appropriate, with post hoc analysis using Fisher's exact test (Statview 4.02, SAS Institute, Cary, NC, USA).

Supplemental Data

Supplemental Data include six figures and Supplemental Results and Supplemental Experimental Procedures, and can be found with this article online at http://www.cancercell.org/cgi/content/full/11/1/37/DC1/.

ACKNOWLEDGMENTS

This study was funded by grants from the Canadian Institutes for Health Research (CIHR), Alberta Heritage Foundation for Medical Research (AHFMR), and Canadian Foundation for Innovation to E.D.M. S.B. is supported by postdoctoral fellowships from both the CIHR and AHFMR.

Received: November 25, 2005
Revised: July 12, 2006
Accepted: October 18, 2006
Published: January 15, 2007

REFERENCES

Andersson, B., Janson, V., Behnam-Motlagh, P., Henriksson, R., and Grankvist, K. (2006). Induction of apoptosis by intracellular potassium ion depletion: using the fluorescent dye PBFI in a 96-well plate method in cultured lung cancer cells. Toxicol. In Vitro *20*, 986–994.

Aramburu, J., Yaffe, M.B., Lopez-Rodriguez, C., Cantley, L.C., Hogan, P.G., and Rao, A. (1999). Affinity-driven peptide selection of an NFAT inhibitor more selective than cyclosporin A. Science *285*, 2129–2133.

Bao, L., Avshalumov, M.V., and Rice, M.E. (2005). Partial mitochondrial inhibition causes striatal dopamine release suppression and medium spiny neuron depolarization via H_2O_2 elevation, not ATP depletion. J. Neurosci. *25*, 10029–10040.

Barrientos, A., and Moraes, C. (1999). Titrating the effects of mitochondrial complex I impairment in the cell physiology. J. Biol. Chem. *274*, 16188–16197.

Bowker-Kinley, M.M., Davis, W.I., Wu, P., Harris, R.A., and Popov, K.M. (1998). Evidence for existence of tissue-specific regulation of the mammalian pyruvate dehydrogenase complex. Biochem. J. *329*, 191–196.

Brandes, R., and Bers, D.M. (1996). Increased work in cardiac trabeculae causes decreased mitochondrial NADH fluorescence followed by slow recovery. Biophys. J. *71*, 1024–1035.

Brandt, U. (2006). Energy converting NADH:quinone oxidoreductase (complex I). Annu. Rev. Biochem. *75*, 69–92.

Caouette, D., Dongmo, C., Berube, J., Fournier, D., and Daleau, P. (2003). Hydrogen peroxide modulates the Kv1.5 channel expressed in a mammalian cell line. Naunyn Schmiedebergs Arch. Pharmacol. *368*, 479–486.

Chen, L.B. (1988). Mitochondrial membrane potential in living cells. Annu. Rev. Cell Biol. *4*, 155–181.

Clayton, R., Clark, J.B., and Sharpe, M. (2005). Cytochrome *c* release from rat brain mitochondria is proportional to the mitochondrial functional deficit: implications for apoptosis and neurodegenerative disease. J. Neurochem. *92*, 840–849.

Dietl, P., Haller, T., Wirleitner, B., Volkl, H., Friedrich, F., and Striessnig, J. (1995). Activation of L-type Ca^{2+} channels after purinoceptor stimulation by ATP in an alveolar epithelial cell (L2). Am. J. Physiol. *269*, L873–L883.

Dohi, T., Beltrami, E., Wall, N.R., Plescia, J., and Altieri, D.C. (2004). Mitochondrial survivin inhibits apoptosis and promotes tumorigenesis. J. Clin. Invest. *114*, 1117–1127.

Don, A.S., and Hogg, P.J. (2004). Mitochondria as cancer drug targets. Trends Mol. Med. *10*, 372–378.

Elstrom, R.L., Bauer, D.E., Buzzai, M., Karnauskas, R., Harris, M.H., Plas, D.R., Zhuang, H., Cinalli, R.M., Alavi, A., Rudin, C.M., and Thompson, C.B. (2004). Akt stimulates aerobic glycolysis in cancer cells. Cancer Res. *64*, 3892–3899.

Eng, J., Lynch, R.M., and Balaban, R.S. (1989). Nicotinamide adenine dinucleotide fluorescence spectroscopy and imaging of isolated cardiac myocytes. Biophys. J. *55*, 621–630.

Gatenby, R.A., and Gillies, R.J. (2004). Why do cancers have high aerobic glycolysis? Nat. Rev. Cancer *4*, 891–899.

Granville, D.J., and Gottlieb, R.A. (2003). The mitochondrial voltage-dependent anion channel (VDAC) as a therapeutic target for initiating cell death. Curr. Med. Chem. *10*, 1527–1533.

Heerdt, B.G., Houston, M.A., and Augenlicht, L.H. (2005). The intrinsic mitochondrial membrane potential of colonic carcinoma cells is linked to the probability of tumor progression. Cancer Res. *65*, 9861–9867.

Kim, J.W., and Dang, C.V. (2005). Multifaceted roles of glycolytic enzymes. Trends Biochem. Sci. *30*, 142–150.

Knoechel, T.R., Tucker, A.D., Robinson, C.M., Phillips, C., Taylor, W., Bungay, P.J., Kasten, S.A., Roche, T.E., and Brown, D.G. (2006). Regulatory roles of the N-terminal domain based on crystal structures of human pyruvate dehydrogenase kinase 2 containing physiological and synthetic ligands. Biochemistry *45*, 402–415.

Komarova, S.V., Pereverzev, A., Shum, J.W., Sims, S.M., and Dixon, S.J. (2005). Convergent signaling by acidosis and receptor activator of NF-κB ligand (RANKL) on the calcium/calcineurin/NFAT pathway in osteoclasts. Proc. Natl. Acad. Sci. USA *102*, 2643–2648.

Koukourakis, M.I., Giatromanolaki, A., Sivridis, E., Gatter, K.C., and Harris, A.L. (2005). Pyruvate dehydrogenase and pyruvate dehydrogenase kinase expression in non small cell lung cancer and tumor-associated stroma. Neoplasia *7*, 1–6.

Kushnareva, Y., Murphy, A.N., and Andreyev, A. (2002). Complex I-mediated reactive oxygen species generation: modulation by cytochrome *c* and NAD(P)+ oxidation-reduction state. Biochem. J. *368*, 545–553.

Levitan, E.S., Gealy, R., Trimmer, J.S., and Takimoto, K. (1995). Membrane depolarization inhibits Kv1.5 voltage-gated K^+ channel gene transcription and protein expression in pituitary cells. J. Biol. Chem. *270*, 6036–6041.

Macian, F. (2005). NFAT proteins: key regulators of T-cell development and function. Nat. Rev. Immunol. *5*, 472–484.

McMurtry, M.S., Bonnet, S., Wu, X., Dyck, J.R., Haromy, A., Hashimoto, K., and Michelakis, E.D. (2004). Dichloroacetate prevents and reverses pulmonary hypertension by inducing pulmonary artery smooth muscle cell apoptosis. Circ. Res. *95*, 830–840.

McMurtry, M.S., Archer, S.L., Altieri, D.C., Bonnet, S., Haromy, A., Harry, G., Bonnet, S., Puttagunta, L., and Michelakis, E.D. (2005). Gene therapy targeting survivin selectively induces pulmonary vascular apoptosis and reverses pulmonary arterial hypertension. J. Clin. Invest. *115*, 1479–1491.

Michelakis, E.D., Hampl, V., Nsair, A., Wu, X., Harry, G., Haromy, A., Gurtu, R., and Archer, S.L. (2002). Diversity in mitochondrial function explains differences in vascular oxygen sensing. Circ. Res. *90*, 1307–1315.

Michelakis, E.D., Thebaud, B., Weir, E.K., and Archer, S.L. (2004). Hypoxic pulmonary vasoconstriction: redox regulation of O_2-sensitive K^+ channels by a mitochondrial O_2-sensor in resistance artery smooth muscle cells. J. Mol. Cell. Cardiol. *37*, 1119–1136.

Namgaladze, D., Shcherbyna, I., Kienhofer, J., Hofer, H.W., and Ullrich, V. (2005). Superoxide targets calcineurin signaling in vascular endothelium. Biochem. Biophys. Res. Commun. *334*, 1061–1067.

Pastorino, J.G., Hoek, J.B., and Shulga, N. (2005). Activation of glycogen synthase kinase 3β disrupts the binding of hexokinase II to mitochondria by phosphorylating voltage-dependent anion channel and potentiates chemotherapy-induced cytotoxicity. Cancer Res. *65*, 10545–10554.

Pitkanen, S., and Robinson, B.H. (1996). Mitochondrial complex I deficiency leads to increased production of superoxide radicals and induction of superoxide dismutase. J. Clin. Invest. *98*, 345–351.

Plas, D.R., and Thompson, C.B. (2002). Cell metabolism in the regulation of programmed cell death. Trends Endocrinol. Metab. *13*, 75–78.

Pozeg, Z.I., Michelakis, E.D., McMurtry, M.S., Thebaud, B., Wu, X.C., Dyck, J.R., Hashimoto, K., Wang, S., Moudgil, R., Harry, G., et al. (2003). In vivo gene transfer of the O_2-sensitive potassium channel Kv1.5 reduces pulmonary hypertension and restores hypoxic pulmonary vasoconstriction in chronically hypoxic rats. Circulation *107*, 2037–2044.

Preussat, K., Beetz, C., Schrey, M., Kraft, R., Wolfl, S., Kalff, R., and Patt, S. (2003). Expression of voltage-gated potassium channels Kv1.3 and Kv1.5 in human gliomas. Neurosci. Lett. *346*, 33–36.

Pu, W.T., Ma, Q., and Izumo, S. (2003). NFAT transcription factors are critical survival factors that inhibit cardiomyocyte apoptosis during phenylephrine stimulation in vitro. Circ. Res. *92*, 725–731.

Remillard, C.V., and Yuan, J.X. (2004). Activation of K^+ channels: an essential pathway in programmed cell death. Am. J. Physiol. Lung Cell. Mol. Physiol. *286*, L49–L67.

Rossow, C.F., Minami, E., Chase, E.G., Murry, C.E., and Santana, L.F. (2004). NFATc3-induced reductions in voltage-gated K^+ currents after myocardial infarction. Circ. Res. *94*, 1340–1350.

Saddik, M., Gamble, J., Witters, L.A., and Lopaschuk, G.D. (1993). Acetyl-CoA carboxylase regulation of fatty acid oxidation in the heart. J. Biol. Chem. *268*, 25836–25845.

Schon, E.A., and Manfredi, G. (2003). Neuronal degeneration and mitochondrial dysfunction. J. Clin. Invest. *111*, 303–312.

Shimizu, S., Narita, M., and Tsujimoto, Y. (1999). Bcl-2 family proteins regulate the release of apoptogenic cytochrome *c* by the mitochondrial channel VDAC. Nature *399*, 483–487.

Stacpoole, P.W. (1989). The pharmacology of dichloroacetate. Metabolism *38*, 1124–1144.

Stacpoole, P.W., Lorenz, A.C., Thomas, R.G., and Harman, E.M. (1988). Dichloroacetate in the treatment of lactic acidosis. Ann. Intern. Med. *108*, 58–63.

Stacpoole, P.W., Nagaraja, N.V., and Hutson, A.D. (2003). Efficacy of dichloroacetate as a lactate-lowering drug. J. Clin. Pharmacol. *43*, 683–691.

Stacpoole, P.W., Kerr, D.S., Barnes, C., Bunch, S.T., Carney, P.R., Fennell, E.M., Felitsyn, N.M., Gilmore, R.L., Greer, M., Henderson, G.N., et al. (2006). Controlled clinical trial of dichloroacetate for treatment of congenital lactic acidosis in children. Pediatrics *117*, 1519–1531.

Vander Heiden, M.G., Chandel, N.S., Schumacker, P.T., and Thompson, C.B. (1999). Bcl-xL prevents cell death following growth factor withdrawal by facilitating mitochondrial ATP/ADP exchange. Mol. Cell *3*, 159–167.

Wang, Z. (2004). Roles of K^+ channels in regulating tumour cell proliferation and apoptosis. Pflugers Arch. *448*, 274–286.

Wang, H., Zhang, Y., Cao, L., Han, H., Wang, J., Yang, B., Nattel, S., and Wang, Z. (2002). HERG K^+ channel, a regulator of tumor cell apoptosis and proliferation. Cancer Res. *62*, 4843–4848.

Warburg, O. (1930). Ueber den stoffwechsel der tumoren (London: Constable).

Yu, S.P., Yeh, C.H., Sensi, S.L., Gwag, B.J., Canzoniero, L.M., Farhangrazi, Z.S., Ying, H.S., Tian, M., Dugan, L.L., and Choi, D.W. (1997). Mediation of neuronal apoptosis by enhancement of outward potassium current. Science *278*, 114–117.

Zamzami, N., and Kroemer, G. (2001). The mitochondrion in apoptosis: how Pandora's box opens. Nat. Rev. Mol. Cell Biol. *2*, 67–71.